Communications Biology

https://doi.org/10.1038/s42003-026-09840-3

Article in Press

Resolvin D1 requires TLR2-FPR2 crosstalk for inflammation resolution and protection during ocular bacterial infection

Received: 28 April 2025

Accepted: 27 February 2026

Cite this article as: Singh, P.K., Singh, S., Kumar, A. *et al.* Resolvin D1 requires TLR2-FPR2 crosstalk for inflammation resolution and protection during ocular bacterial infection. *Commun Biol* (2026). https://doi.org/10.1038/s42003-026-09840-3

Pawan Kumar Singh, Sukhvinder Singh, Ajay Kumar, Shailendra Giri & Ashok Kumar

Resolvin D1 requires TLR2-FPR2 crosstalk for inflammation resolution and protection during ocular bacterial infection

Authors:

Pawan Kumar Singh[1*], Sukhvinder Singh[1], Ajay Kumar[1], Shailendra Giri[2], and Ashok Kumar[1,3 #]

Affiliations:

[1]Department of Ophthalmology, Visual and Anatomical Sciences, Wayne State University School of Medicine, Detroit, MI, USA

[2]Department of Neurology, Henry Ford Health System, Detroit, MI, USA

[3]Department of Biochemistry, Microbiology, and Immunology, Wayne State University School of Medicine, Detroit, MI, USA

*Current affiliation: Department of Ophthalmology, Mason Eye Institute, University of Missouri School of Medicine, Columbia, Missouri, USA.

 # Corresponding Author

Ashok Kumar, Ph.D.

Department of Ophthalmology, Visual, and Anatomical Sciences

Wayne State University School of Medicine

4717 St. Antoine, Detroit, MI 48201, USA

Tel: (313) 577-6213

E-mail: akuma@med.wayne.edu

Abstract

The eye is highly susceptible to inflammation-induced tissue damage; however, the mechanisms that drive inflammation resolution during ocular infections remain unclear. In this study, we utilize a murine model of intraocular bacterial infection (*S. aureus*-induced endophthalmitis) and lipidomic analysis to uncover a critical role of pro-resolving lipid mediators, particularly resolvin D1 (RvD1), in resolving inflammation and restoring ocular tissue homeostasis and vision. RvD1 protects mouse eyes from severe endophthalmitis by enhancing bacterial clearance, suppressing intraocular inflammation, and preserving retinal structure and function. Pharmacological inhibition of formyl peptide receptor 2 (FPR2) reveals that RvD1's protective effects mainly rely on FPR2 signaling. Unexpectedly, RvD1 is unable to resolve inflammation or protect the eye in the absence of Toll-like receptor 2 (TLR2), a critical pattern recognition receptor in ocular *S. aureus* infections. These findings reveal an unrecognized interplay between TLR2 and FPR2 signaling, including their mutual regulation and physical receptor interactions during bacterial infection. Overall, these findings provide new insights into the coordinated roles of TLR2 and FPR2 in resolving inflammation and protecting the eye during bacterial infections.

Keywords: *S. aureus*, Eye, Endophthalmitis, Inflammation, RvD1, TLR2, FPR2.

Introduction

Ocular infections, especially bacterial endophthalmitis, remain a potentially blinding eye disease, which occurs due to the post-operative, post-traumatic, or endogenous inoculation of bacteria into the eye[1, 2]. Despite therapeutic and surgical interventions, endophthalmitis results in partial to complete vision loss in many patients[3]. Over the past two decades, the incidence of bacterial endophthalmitis has risen steadily, primarily due to the increased popularity of sutureless cataract surgery[4], small-gauge vitrectomy[5], and intravitreal injections of anti-VEGF drugs for the treatment of retinal diseases[6]. Severe vision loss in endophthalmitis is a cumulative effect of pathogen virulence factors, such as toxins[3, 7] and an uncontrolled or unresolved inflammatory response leading to ocular tissue damage[8]. Unfortunately, the current treatment for bacterial endophthalmitis mainly involves the intravitreal injection of antibiotics, which, while killing bacteria, do little to suppress ongoing inflammation[8]. Thus, it is of paramount importance to uncover newer therapeutics to treat endophthalmitis, such as anti-inflammatory agents that may be used alone or in combination with antibiotics and are preferably non-immunosuppressive[9, 10].

The resolution of inflammation is an active and highly regulated process that restores tissue homeostasis without compromising host defense[11]. One of the mechanisms underlying inflammation resolution is the lipid mediators class switch, where eicosanoids such as prostaglandins (PGs) and leukotrienes (LTs) are produced during the onset of inflammation, and later on, cells switch to synthesizing specialized pro-resolving mediators (SPMs)[12]. These SPMs include resolvins, protectins, maresins, and lipoxins[12], which actively promote the cessation of neutrophil recruitment, stimulate macrophage efferocytosis (clearance of apoptotic cells), and support tissue repair during bacterial

infection[13]. Resolvins are derived from ω-3 polyunsaturated fatty acids (PUFAs) and broadly classified as either 'D' or 'E' series resolvins. D resolvins are synthesized from docosahexaenoic acid (DHA) metabolism by 5-lipoxygenase (5-LOX) and 15-lipoxygenase (15-LOX), whereas E-series resolvins are produced from eicosapentaenoic acid (EPA) by a series of enzymatic actions (cytochrome p450, aspirin-acetylated cyclooxygenase-2 (COX-2) and 5-LOX) [14,15]. Protectins and maresins are also ω-3 PUFA derivatives generated from DHA through the 15-LOX and 12-LOX mediated pathways, respectively[16, 17]. These SPMs exert pro-resolving activities via multiple mechanisms such as reduced neutrophil recruitment[16, 18] and increased phagocytosis of apoptotic neutrophils, tumor cell debris, and live bacteria[19, 20]. Additionally, they impair T-cell migration[21], reduce pro-inflammatory cytokines and chemokines[22, 23], alleviate oxidative stress[24], and promote wound healing[25, 26]. The pro-resolution effects of these lipid mediators have been investigated in several infectious disease models (reviewed in[12]), including pulmonary inflammation[27], bacterial pneumonia and acute lung injury[28, 29], burn-related sepsis[30], neuroinflammation[31], neuropathic pain[32], periodontitis[33] periodontal wound healing [34], herpetic keratitis[18], and influenza virus infection[35]. At the molecular level, SPMs exert their pro-resolving actions via activating specific G-protein coupled receptors (GPCRs)[36]. Among these GPCRs, human ALX/FPR2 has been shown to bind multiple SPMs, including RvD1, and has been extensively studied in the context of inflammation resolution.

The immunomodulatory properties of SPMs have not been investigated in ocular bacterial infections, particularly bacterial endophthalmitis. Therefore, we performed untargeted lipidomics analysis to assess the temporal changes in total lipids and oxylipins in *S.*

aureus-infected mouse retinas and cultured bone marrow-derived macrophages (BMDMs), which revealed significant alterations in lipid profiles[37]. To further investigate the functional role of lipids in bacterial endophthalmitis, here, we performed targeted lipidomic analysis and observed the production of several specialized pro-resolving mediators (SPMs), including RvD1, in the infected mouse retina. This prompted us to examine the immunomodulatory role of RvD1 and elucidate the mechanisms underlying its pro-resolving properties. Alongside demonstrating RvD1's protective effects, our study revealed a previously unrecognized interplay between FPR2 and TLR2, which is critical for coordinating the pro-resolving properties of RvD1.

Results

Bacterial infection increases SPM production in the mouse retina.

Our prior study demonstrated significant metabolic perturbations in the retinal tissue during endophthalmitis[9]. Given the critical role of lipids in regulating inflammatory responses during infection, we reanalyzed the metabolomics data with a focus on lipid metabolism. We found that *S. aureus* infection altered polyunsaturated fatty acid (PUFA) metabolism in the retina, with a significant increase in both omega-3 (n3) and omega-6 (n6) PUFAs **(Fig. 1A, and S1)**. Additional fatty acids that showed substantial temporal changes in the infected retina included docosatrienoate, docosadienoate, erucate, nervonate, and dihomo-linoleate. A time-dependent increase in lysolipids and monoacylglycerols accompanied these increases. These lipid fragments, generated through lipase-mediated hydrolysis of phospholipids and triglycerides, indicate the

breakdown of complex lipids. Pathway enrichment analysis further revealed dysregulation of lipid metabolism with linoleic acid metabolism as one of the top altered metabolic pathways (**Fig. 1B and Table S1)**, which can contribute to the production of specialized pro-resolving mediators (SPMs) during inflammation[38].

To investigate the dynamics of endogenously produced SPMs during endophthalmitis, we conducted a lipidomic analysis. Temporal LC-MS profiling of *S. aureus*-infected retinal tissue revealed changes in approximately 130 lipid mediators derived from linoleate, arachidonate, eicosapentaenoate, and docosahexaenoate. These mediators exhibited either pro-inflammatory [e.g., 5-HETE (5-hydroxy eicosatetraenoic acid), 9-HODE (9-hydroxy octadecadienoic acid), PGE_2 (prostaglandin E2)] or anti-inflammatory properties [e.g., 12-HETE (12-hydroxy eicosatetraenoic acid), 4-HDoHE (4- hydroxy docosahexaenoic acid), 7-HDoHE (7-hydroxy docosahexaenoic dcid,14HDoHE (14-hydroxy-docosahexaenoic acid)] **(Fig. 1C).** The presence of SPMs was further validated by intravitreal supplementation of DHA in infected eyes. Our data demonstrated increased production of several SPMs and their precursors, including RvD1, RvD5, LXA_4, 7-HDoHE, 4-HDoHE, 8-Oxo-RvD1, RvE3, PD1, 17-HDoHE, and 14-HDoHE. Notably, DHA supplementation further enhanced the levels of select metabolites **(Fig. 1D)**. Together, these results indicate that lipid metabolism is markedly altered during ocular infections and inflammation, contributing to the production of pro-resolving lipid mediators.

RvD1 treatment ameliorates bacterial endophthalmitis and preserves vision.

Our lipidomic analysis showed the production of several SPMs in infected retinal tissue; next, we sought to examine their functional roles during endophthalmitis. As SPMs are

known to exert pro-resolving effects, we tested the effects of RvD1, RvD2, RvD5, PD1, and LXA4 by intravitreal injections in *S. aureus*-infected mouse eyes and measured IL-1β levels, a key inflammatory cytokine produced during endophthalmitis in mice[39] and humans[40]. Our results show that all SPMs significantly diminished IL-1β levels, with RvD1 exhibiting marked reduction (**Fig. 2A**). Therefore, we chose to investigate the role of RvD1 in resolving retinal inflammation during infection, which has yet to be explored. We used both prophylactic and therapeutic approaches by giving intravitreal injections of RvD1 (10 ng/eye) prior to or post-*S. aureus* infection as per the timeline shown in **Fig. 2B**. To this end, our results show that RvD1 treatment (both pre- and post-) drastically diminished corneal haze and opacity **(Fig. 2C)**, preserved retinal integrity and architecture **(Fig 2D),** resulting in reduced clinical scores **(Fig. 2E)**. We also measured intraocular bacterial burden in SA-infected and RvD1-treated eyes and observed a significant decline in RvD1 treated eyes in all experimental groups **(Fig. 2F)**. Consistent with our prior studies[41 42], retinal tissue damage during endophthalmitis coincided with reduced retinal function as assessed by scotopic ERG response, showing decreased amplitudes of a and b-waves in SA-infected eye. However, RvD1-treated eyes had significant retinal function with ~80% retention of both a-waves and b-waves amplitudes **(Fig. 2G)**, indicating its protective role.

RvD1 reduces inflammation and promotes M1-to-M2 macrophage polarization.

Intraocular inflammation is one of the hallmarks of bacterial endophthalmitis. Although essential, uncontrolled inflammation in the eye causes more tissue damage than the pathogen itself. Consistent with the known pro-resolving properties of SPMs, we assessed the effect of RvD1 on the inflammatory cytokine/chemokine production in the

eyes using qPCR and ELISA. Our results show that SA infection significantly increased retinal inflammation, whereas pre- or post-RvD1 treatment markedly reduced the SA-induced inflammatory response, as evidenced by decreased transcript levels of *Il-1β, Il-6, Tnf-α*, *Cxcl-2,* and *Cxcl-1* genes (**Fig. 3A and S2).** Our ELISA results further confirmed that the RvD1 treatment decreased the protein levels of these inflammatory mediators (**Fig. 3B and S2)**.

Our prior studies reported that increased production of cytokines and chemokines recruits PMNs, which constitute the predominant innate immune cell type during endophthalmitis [10]. However, persistent PMN infiltration causes irreversible ocular tissue damage in the eye[43, 44]. To determine the effect of RvD1 on PMNs, flow cytometry (**Fig. 3C)** was performed, and observed PMN levels were significantly reduced in all RvD1-treated eyes (**Fig. 3D**). These findings highlight the pro-resolving effects of RvD1 and indicate that a delicate balance in the inflammatory response and immune cell infiltration is essential to protect the eye during infection.

One of the potential mechanisms underlying RvD1 pro-resolving activity is enhancing the production of anti-inflammatory molecules and inducing class switching of the macrophages/microglia from inflammatory (M1) towards anti-inflammatory (M2) phenotype[45]. Thus, we checked the expression of various anti-inflammatory molecules via qPCR and observed that RvD1 treatment enhanced the expression of *Il-4, Il-10*, and *Tgf-β1* in retinal tissue **(Fig. 4A)**. Moreover, RvD1 treated retinal tissue exhibited reduced level of M1 markers, *iNOS, IL-23p19*, and *IL-12p40* **(Fig. 4B)** and higher expression of M2 markers, *Arg-1*, *Fizz-1*, and *Ym-1* **(Fig. 4C)**. These results suggest that RvD1

promotes the class switching of macrophages/microglia from a pro-inflammatory, M1 phenotype to an anti-inflammatory/pro-resolving M2 phenotype.

M2 milieu in eye resulting in enhanced inflammation resolution and protection.

TLR2 deficiency diminishes RvD1 treatment efficacy during endophthalmitis

Previously, we demonstrated that *S. aureus* activates innate immune signaling in the eye via TLR2[46, 47], and that its deficiency increases disease severity due to increased bacterial burden and persistent inflammation[44]. Thus, we hypothesized that RvD1 could accelerate inflammation resolution and reduce disease severity in TLR2 knockout mice. So, similar to our WT mice, we treated the TLR2$^{-/-}$ infected mice with RvD1 by intravitreal injections at pre (-12h) and post (+6h and +12h) *S. aureus* infections. Unexpectedly, RvD1 treatment failed to rescue TLR2$^{-/-}$ mice from endophthalmitis, as evidenced by comparable corneal haze and opacity in treated vs untreated groups **(Fig. 5A)**. Moreover, RvD1 had no effect in reducing bacterial burden **(Fig. 5B)** and preserving retinal tissue integrity (**Fig. 5C**) in any experimental groups. Similarly, the levels of inflammatory mediators **(Fig. 5D and S3)** and PMN infiltration **(Fig. 5E&F)** remain unaffected by RvD1 treatment. Together, these results indicate that the pro-resolving effects of RvD1 require TLR2 signaling.

RvD1 increases FPR2 expression in wild-type but not in TLR2$^{-/-}$ mouse retina

RvD1 acts through GPCRs ALX/FPR2 to promote inflammation resolution[48]. FPR2 is predominantly expressed in myeloid cells, with lower expression observed in lymphocytes, dendritic cells, and endothelial cells[49]. Earlier, we reported that both microglia and Müller glia play a role in TLR2-mediated retinal innate response during *S.*

aureus infection[47, 50]. Therefore, we assessed PR2 expression *in vitro* (**Fig. 6A, left panels**) using mouse microglial (BV2 cell line) and human Müller glia (MIO-M1 cell line) and *in vivo* in mouse retinal tissue (**Fig. 6A, right panels**) using cell-specific markers. Our results show that both microglia and Müller glia express FPR2. To determine whether RvD1 treatment influences FPR2 levels, we examined FPR2 expression in the retina of WT and TLR2$^{-/-}$ mice, considering the differences in RvD1-mediated resolution and protection. Interestingly, our results show that RvD1 treatment significantly upregulated *Fpr2* expression in WT mice at transcript (**Fig. 6B**) and protein levels (**Fig. 6C**). In contrast, no significant increase in FPR2 expression was observed by RvD1 treatment in TLR2$^{-/-}$ mice, either at transcript **(Fig. 6B)** or protein **(Fig. 6C)** levels. This data suggests an intricate relationship between TLR2 and FPR2 signaling in response to RvD1 treatment in the eye.

FPR2 inhibition abolishes pro-resolving and antibacterial properties of RvD1

RvD1 is known to signal through FPR2, and our findings further support this, demonstrating increased FPR2 expression in RvD1-treated wild-type mouse retinal tissue. However, the precise role of FPR2 during *S. aureus* endophthalmitis remains unexplored. To investigate this, we intravitreally injected mice with two different FPR2 antagonists, PBP10 or WRW4, 12h before bacterial infection. Subsequently, eyes were injected with *S. aureus,* and RvD1 treatment was given at 6h post-infection, similar to prior experiments. Eyes without RvD1 treatment were used as disease control, and those treated with WRW4 or PBP10 and *S. aureus* infection were used as inhibitor controls. Our data show that pretreatment with FPR2 antagonists diminished RvD1-mediated

protection, resulting in increased bacterial burden **(Fig. 7A)**, inflammatory mediators **(Fig. 7B),** and PMN infiltration **(Fig. 7C & D)**.

In addition to reducing inflammation, our data consistently showed reduced bacterial burden in RvD1-treated eyes. To investigate the potential antibacterial mechanisms, first, we incubated *S. aureus* with different concentrations of RvD1, followed by a bacterial plate count, and concluded that RvD1 does not exert direct antibacterial activity (data not shown). Next, we postulated that RvD1 could enhance the bacterial phagocytic and killing activity of retinal resident cells or infiltrating innate immune cells. To test this hypothesis, we used human retinal Müller glia, which we have previously demonstrated kill *S. aureus* via phagocytosis[50] or the production of antimicrobial peptides[51]. Our data showed that RvD1 pretreatment of Müller glia enhanced the phagocytosis **(Fig. 7E)** and intracellular killing **(Fig. 7F)** of *S. aureus*. Moreover, these antibacterial activities were diminished in the presence of FPR2 antagonists, PBP10 or WRW4. Taken together, these findings underscore the pivotal role of FPR2 in orchestrating the anti-inflammatory and antibacterial actions of RvD1 during bacterial endophthalmitis.

TLR2 and FPR2 engage in mutual regulation and direct physical interaction

Intrigued by the inability of RvD1 to confer protection in $TLR2^{-/-}$ mice and enhanced expression of FPR2 in wild-type but not in $TLR2^{-/-}$ mice retina led us to investigate the intricate relationship between TLR2 and FPR2. First, we checked their mutual expression in the mouse retina by pharmacological activation and inhibition studies in wild-type mice by intravitreal injections of TLR2 agonist (Pam3), TLR2 neutralizing antibody, FPR2 agonist (WKYMVM), or FPR2 antagonist (PBP10), either alone or in combination where inhibitors were injected 12h before their respective activators. Our qPCR data show that

Pam3 significantly upregulated the expression of FPR2, and its expression was comparable to that of WKYMVM-treated retinal tissue **(Fig. 8A)**. Similarly, WKYMVM treatment significantly increased TLR2 mRNA expression **(Fig. 8B)**. However, the blockade of TLR2 receptor using an anti-TLR2 neutralizing antibody or inhibition of FPR2 by PBP10 attenuated the expression of Fpr2 and *Tlr2*, respectively **(Fig. 8A&B)**. Thus, the activation or inhibition of TLR2 influences FPR2 expression and vice versa.

Next, we sought to investigate if there is any physical interaction between these two receptors. To address this question, we performed co-immunoprecipitation assays in HEK293 cells transfected with plasmid constructs of *Tlr2-HA* and *Fpr2-FLAG* genes and using anti-HA (TLR2) and anti-FLAG (FPR2) antibodies, followed by Western blot using anti-HA antibody. Control experiments using IgG and A/G beads ruled out nonspecific pull-downs. Our results show crosstalk between TLR2 and FPR2 receptors as revealed by co-immunoprecipitation(co-IP) of FLAG-FPR2 with an HA-TLR2 antibody and vice versa **(Fig. 8C)**. To further validate the interaction between TLR2 and FPR2 during endophthalmitis, we performed a co-IP assay using anti-TLR2 and anti-FPR2 antibodies on retinal lysates obtained from *S. aureus*-infected eyes, both with (+6h) and without RvD1 treatment. Co-IP revealed the association of TLR2 with FPR2 in infected retinal lysates and in RvD1-treated samples, substantiating the *in vivo* interaction of these receptors (**Fig. 8D)**. These findings demonstrate that TLR2 and FPR2 exhibit a reciprocal regulatory relationship, with each receptor influencing their expression and physical interactions with the other, indicating their interdependency in RVD1-mediated inflammation resolution and protective effects in the eye.

Discussion

Being an immune-privileged organ, the eye is especially susceptible to tissue damage caused by excessive inflammation; however, the mechanisms involved in resolving inflammation during ocular infections remain poorly understood. Thus, the long-term goal of our research has been to uncover newer immunomodulatory therapeutics that can be used alone or in combination with an antibiotic to minimize inflammation-mediated tissue damage in the eye [9, 52]. Here, in this study using metabolomics and lipidomic approaches, we demonstrate the role of SPMs, especially RvD1, in promoting inflammation resolution and protecting the eye during bacterial endophthalmitis. Notably, we uncovered that in addition to its known receptor, FPR2, RvD1-mediated inflammation resolution needs TLR2 signaling, as TLR2 deficiency diminishes the protective effects of RvD1. Collectively, our study highlights a previously unknown interaction between TLR2 and FPR2 in regulating inflammatory responses in the eye.

Our interest in the mechanisms of inflammation resolution during ocular infection originated from the observation that TLR2 ligand treatment attenuated *S. aureus*-induced inflammation and protected the mice from severe endophthalmitis[41]. Moreover, deficiency of TLR2 and its downstream adaptor MyD88 rendered the mice more susceptible to endophthalmitis, indicative of the protective role of the TLR2→MyD88 signaling axis[44]. We reasoned that reduced inflammation and functional recovery of the retina following *S. aureus* infection might be related to the endogenous production of bioactive lipid mediators, such as lipoxins, resolvins, and protectins, collectively termed SPMs[12] and that TLR2 regulates their production and/or signaling. SPMs are endogenously produced molecules that actively promote inflammation resolution. In recent years, SPMs have

attained more attention as novel therapeutic targets in various infectious and inflammatory diseases[53, 54]. These mediators are produced in response to infection and/or inflammation and secreted into the cellular milieu, functioning in both an autocrine and paracrine manner to control inflammation[55, 56]. Our lipidomics and metabolomics analyses show the production of various SPMs, including RvD1, and their precursors in the retina during bacterial endophthalmitis, implicating their pro-resolving roles during ocular infections. Given that the timely resolution of inflammation is essential to prevent retinal damage, we sought to investigate the protective role of SPMs and determine the underlying mechanisms. In particular, we focused on RvD1, which is known to act via the FPR2 receptor to reduce inflammation and promote tissue repair.

The retinal tissue is full of DHA and acts as the substrate for 5-LOX and 15-LOX enzymes to produce SPMs[48]. We postulated that DHA supplementation would increase the production of SPMs in the retina, resulting in faster resolution in our non-resolving model of *S. aureus* endophthalmitis[44]. Indeed, our data showed increased production of SPMs, RvD1, RvD5, PD1, and LXA4 in DHA-supplemented infected eyes. Moreover, all these SPMs exerted their pro-resolving effects, with RvD1 exhibiting relatively better activity in reducing intraocular inflammation. We found that RvD1 significantly reduced clinical symptoms (corneal haze and opacity) of endophthalmitis in mouse eyes. Our study corroborated the findings where RvD1 has been shown to reduce clinical scores and disease severity in endotoxin-induced uveitis [22 57] and allergic eye disease [58]. Among the SPMs, LXA4, which is structurally similar to RvD1, has been shown to reduce alkali burn-induced corneal inflammation and neovascularization, facilitate corneal wound healing, and modulate pathogenic responses in autoimmune uveitis[59, 60, 61]. Consistent

with this, mice lacking 12/15-LOX exhibit impaired corneal wound repair, likely due to diminished LXA4 production[59]. We have reported a rapid decline in ERG response in bacterial endophthalmitis[41, 50], culminating in impaired or complete vision loss. However, RvD1 treatment maintained retinal functions, which correlated with preserved retinal structural integrity as assessed by histology.

S. aureus infection induces severe inflammation, leading to retinal cell damage[44, 50]. Interestingly, our findings demonstrated that RvD1 effectively diminished *S. aureus*-induced inflammatory cytokines (TNF-α, IL-1β, IL-6). Among chemokines, RvD1 treatment significantly attenuated both CXCL-2 and CXCL-1, wherein CXCL2 has been shown to play a key role in PMN chemotaxis during bacterial endophthalmitis[52, 62]. Our study corroborated with similar findings where RvD1 has been shown to reduce the inflammatory cytokines in pulmonary inflammation[63, 64], peritonitis[26], periodontitis[34], arthritis[65], and endotoxin-induced uveitis[22, 57]. We and others have shown that bacterial infection of the eye leads to severe retinal inflammation with prominent involvement of infiltrating PMNs[44, 66, 67]. Excessive PMN infiltration and impaired neutrophil clearance from the retina can lead to irreversible retinal tissue damage[66, 67]. Here, we report that RvD1 dampens neutrophil recruitment and infiltration in the retina. A similar observation has been reported with other related SPMs, RvE1 and NPD1, in reducing the neutrophil recruitment to the cornea in bacteria and LPS-induced inflammation[68] and HSV-induced keratitis[18], respectively. These findings further emphasize the pro-resolving and tissue-protective properties of RvD1 in regulating ocular inflammation.

Some studies suggest that RvD1 regulates pro and anti-inflammatory miRNAs via G-protein coupled receptor signaling, resulting in increased production of *Il-10* and

reduction of NF-KB pathways[69, 70]. To explore the pro-resolving property of RvD1 during retinal infection/inflammation, we measured the expression of anti-inflammatory mediators. Notably, RvD1 treatment induced the expression of several anti-inflammatory mediators, including *Il-4, Il-10*, and *Tgf-β1*. Our results are consistent with the findings where RvD1 treatments have been reported to increase the production of anti-inflammatory mediators in cigarette smoke-induced lung inflammation[23]. Our recent study demonstrated that AMPK-α-mediated regulation of macrophage phenotypes (M1 to M2 switch) plays a pivotal role in resolving inflammation in bacterial endophthalmitis[10]. Alternatively, activated macrophages (M2) are immunoregulatory cells that have anti-inflammatory properties, and they maintain tissue homeostasis by eliminating tissue debris and apoptotic bodies via phagocytosis[29, 71]. It is well established that IL-4 and IL-10 promote the alternatively activated M2 macrophage phenotype[72]. Here, we showed that RvD1 treatment creates a pro-resolving milieu by inducing M2 macrophages and reducing M1 macrophage phenotype in the retina during *S. aureus* infection. Our finding supports similar findings observed in multiple sclerosis, liver reperfusion injury, cigarette smoke-induced lung inflammation, and uveitis models, where RvD1 has been shown to enhance M2 polarization[23, 45, 57]. These results highlight RvD1's potential to modulate macrophage phenotypes, thereby promoting the resolution of inflammation in the retina during infections.

Previous studies have suggested that resolvins and protectins are part of the antimicrobial defense and enhance bacterial phagocytosis from macrophages and neutrophils without stimulating uncontrolled inflammation and collateral tissue damage or mediating immunosuppression[73, 74, 75]. Our study also corroborated these findings, and

here, we demonstrated that RvD1 antimicrobial effects are mediated by enhanced phagocytosis and intracellular killing of the pathogen by retinal resident Müller glial cells. Our results are also supported by studies indicating resolvins stimulate the phagocytosis of *E. coli*[19] and tumor cell debris[20] by macrophages.

Having established the pro-resolving role of RvD1 in endophthalmitis, we sought to investigate its role in TLR2$^{-/-}$ mice, which exhibit an increased disease severity during *S. aureus* endophthalmitis[44]. We hypothesized that RvD1 treatment would enhance inflammation resolution in these mice. In contrast, we observed that RvD1 failed to protect and exert pro-resolving/anti-inflammatory properties in TLR2$^{-/-}$ mice. Although no reports specifically examine the pro-resolving role of RvD1 in TLR-deficient animal models, a study by Koltsida and co-workers reported that TLR7 activation mediates the production of resolvins and protectins in a mouse model of allergic airway inflammation[76]. These findings suggest an intricate interplay between TLR signaling and SPMs. Some recent studies show that factors regulating inflammation may alter the balance of pro- vs anti-inflammatory signals by regulating FPR2 expression[77]. Additionally, the pro-resolving properties of resolvins are mediated through FPR2[78, 79]. In the current study, we demonstrated that retinal microglia and Muller glia abundantly express the FPR2, and RvD1 treatment potentiates the expression of the FPR2 in WT but not in TLR2$^{-/-}$ mice. Furthermore, blocking the FPR2 receptor in WT mice reversed the anti-bacterial/anti-inflammatory property of RvD1, indicating that both FPR2 and TLR2 receptors are required to mediate the RvD1 pro-resolving action in *S. aureus*-induced retinal inflammation.

Although the role of FPR2 in RvD1-mediated resolution has been documented previously, the role of TLR2 and its interaction with FPR2 in this resolution process has not been explored until now. Here, we demonstrated for the first time that TLR2 activation promotes the expression of FPR2, and vice versa, in the context of retinal inflammation. We also discovered that TLR2 and FPR2 inhibition suppresses the expression of each other. We are intrigued by the observation of why RvD1 failed to protect $TLR2^{-/-}$ mice and how TLR2 and FPR2 influence the expression of each other to mediate the pro-resolving property of RvD1. To our knowledge, our results unravel previously unknown "crosstalk" between TLR2 and FPR2 receptors and highlight that this physical interaction is essential for RvD1 to exert its pro-resolving effects in *S. aureus*-induced retinal inflammation. Although there is no report on crosstalk between FPR2 with any innate immune receptors, particularly with TLR2, our findings provide a mechanistic context for few previous reports showing the activation of TLR2 using TLR2 agonist PGN, Pam3, Pam3CSK4, and a NOD2 ligand MDP in microglial cells resulted in upregulation of mFPR2, and, silencing of TLR2 using siRNA failed to induce the expression of mFPR2[80, 81]. Altogether, our study discovered that TLR2 activation/inhibition regulates the expression of FPR2 and, therefore, may actively participate in both the pathogenic process of inflammation and RvD1-mediated resolution of inflammation.

In summary, our study reveals that a single intravitreal injection of RvD1 efficiently protected the eyes of wild-type mice from bacterial endophthalmitis but failed to do so in TLR2-deficient mice. These findings highlight the potent anti-inflammatory and pro-resolving activity of RvD1 in infectious retinal inflammation. Thus, RvD1 could be a promising anti-inflammatory therapy either alone or in combination with antibiotics for

treating ocular infections. Importantly, we provide the first evidence of a physical and functional crosstalk between TLR2 and FPR2 receptors in mediating RvD1-driven resolution of retinal inflammation.

Methods

Reagents

The TLR2 agonist Pam3CSK4 (cat # tlrl-pms) was purchased from InvivoGen (San Diego, CA). The FPR2 agonist WKYMVM (cat # 1799) and antagonists WRW4 (cat # 2262) and PB10 (cat # 4611) were purchased from Tocris Biosciences (Minneapolis, MN). Anti-TLR2 neutralizing antibody (cat # ab9100) was purchased from Abcam (Cambridge, MA). RvD1, RvD2, RvD5, and LXA4 were purchased from Cayman Chemicals (Ann Arbor, MI). Anti-HA (cat # 05-904, Millipore), anti-FLAG (cat # F1804, Sigma), anti-TLR2 (cat # 13744 Cell Signaling), anti-FPR2 (cat # sc-66901, Santa Cruz Biotechnology), fixable viability dye eFLOUR 660 (cat # 65-0864, Thermo Fisher Scientific), and CD45-PECy5 (cat # 553082), Ly6G-FITC (cat # 561105), purchased from BD Biosciences (San Jose, CA).

Cells and Culture Conditions.

The immortalized human Müller glia cell line MIO-M1 (received from Dr. Astrid Limb, University College, London, UK) and mouse microglia cells, BV2, were maintained in DMEM supplemented with 10% FBS, 1% penicillin-streptomycin and 10 µg/mL L-glutamine. Whenever needed, cells were grown overnight in low serum (1-2%) and antibiotic-free DMEM before infection.

Mice and ethics statement

C57BL/6 (wild type, WT) and TLR2$^{-/-}$ (B57BL/6 background) mice were purchased from Jackson Laboratory (Bar Harbor, ME), and the knockout (KO) mice were bred in-house. Animals were housed in a pathogen-free, restricted-access DLAR facility, maintained under a 12h light: 12h dark cycle, and fed on LabDiet rodent chow (Labdiet Pico lab Laboratory, St Louis, MO) and water *ad libitum*. Both male and female mice, 6-10 weeks of age, were used in all experiments. Animals were euthanized by CO_2 inhalation followed by cervical dislocation at designated experimental endpoints. Mice were treated in compliance with the Association for Research in Vision and Ophthalmology (ARVO) Statement for the Use of Animals in Ophthalmic and Vision Research, and all procedures were approved by the Institutional Animal Care and Use Committee (IACUC) of Wayne State University. We have complied with all relevant ethical regulations for animal use.

Induction of endophthalmitis.

The eyes of C57BL/6 and TLR2$^{-/-}$ mice were intravitreally injected with 1 µl of PBS containing 5000 colony-forming units (CFUs) of *S. aureus* RN6390 to induce endophthalmitis[41, 44, 50]. The RvD1 treatment (10ng/µl/eye) was given 12h prior (prophylactic in group I), 6h post (group II), and 12 h post (group III) *S. aureus* infection as described in the time chart shown in figure 2B. Clinical examinations were performed using an ophthalmoscope mounted with a camera. The ocular disease was graded, and clinical scores from 0 to 4 were assigned using the previously described scale[67, 82]. The clinical score of 4 is considered as 100 percent damage, and based on this, the percent damage and percent retention of eyes were calculated in both RvD1-treated vs. *S. aureus*-infected eyes. At the desired time points post-infection; neuro retina/eyes were subjected to metabolomics, lipidomics, bacterial burden, inflammatory

cytokine/chemokine assays, PMN infiltration, and histology, as described in the following sections.

Metabolomics analysis.

For the metabolomics study, six retinas were pulled together at the desired time points post-infection. The retinal tissues were snap frozen and sent to Metabolon Inc. for extraction and metabolomics analysis. The untargeted metabolomics analysis was performed at Metabolon Inc. (Morrisville, NC).

Sample preparation and LC-MS for lipidomics.

The lipidomic analysis was performed by the Wayne State University lipidomics core. The retinal lysates (pooled 6 retinas) from infected and mock-treated controls were extracted and analyzed by LC-MS to determine fatty acyl lipidome according to previously validated methods[83, 84]. Briefly, retinal lysates (200µl) were spiked with 5 ng each of the internal standards (IS). The samples were diluted to 1 ml with 15% methanol in water and purified using C18 solid-phase extraction cartridges (Strata-X, Phenomenex, Torrance, CA). The cartridges were preconditioned with 1ml methanol followed by 1ml 15% methanol in water. The diluted and IS spiked samples were applied to the C18 cartridge, washed with 2ml of 15% methanol and 2ml hexane, and dried in vacuum for 30 sec. Samples were eluted using 0.5ml methanol containing 0.1% formic acid into 1.5ml LC-MS autosampler vials. The eluate was dried under a gentle stream of nitrogen, reconstituted in 50µl of methanol, and stored at -80°C until LC-MS analysis. Reversed-phase HPLC was performed using C18 column (Luna, C18 (2); 2.1x150 mm, 3µm; Phenomenex), mounted on the Prominence XR HPLC system (Shimadzu, Kyoto, Japan). The mobile phase consisted of a gradient between solution A, methanol-water-acetonitrile (10:85:5 v/v/v),

and solution B, methanol-water-acetonitrile (90:5:5 v/v/v), both containing 0.1% ammonium acetate. The gradient program with respect to the composition of solution B was as follows: 0-1 min, 50%; 1-8 min, 50-80%; 8-15 min, 80-95%; and 15-17 min, 95%. The flow rate was 0.2 ml/min. The HPLC column was fully equilibrated to initial conditions before each sample was injected. The HPLC eluate was directly introduced to the electrospray ionization source (TurboV) of the QTrap5500 mass analyzer (AB Sciex, Framingham, MA, USA) in the negative ion mode with the following settings: curtain gas, 35 psi; GS1, 35 psi; GS2, 65 psi; temperature, 600°C; ion spray voltage, -1500 V; collision gas, low; declustering potential, -60 V; and entrance potential, -7 V. The eluate was monitored by the multiple reaction monitoring (MRM) method, to detect unique molecular ion-daughter ion combinations for each of the 60 transitions (to monitor a total of 69 lipid mediators from arachidonic acid metabolism with 8 ms dwell time for each transition and 5 ms settling time between scans. The total cycle time was 1.625s. Optimized collisional energies (18-35 eV) and collision cell exit potentials (7-10 V) were used for each MRM transition. The data were collected with Analyst 1.5.2 software (AB Sciex), and the MRM transition chromatograms were quantified by MultiQuant software (AB Sciex). The IS signals in each chromatogram were used for normalization, recovery, and relative quantitation of each analyte. The concentration of each detected analyte in the retinal lysate was calculated by dividing the detected quantities [in nanograms (ng)] with their corresponding total protein quantity and reported as ng/mg protein.

Bacterial burden estimation

The bacterial burdens in the infected/RvD1-treated eyes were determined using the standard bacterial plate count method [44, 50]. Briefly, at the desired time points, the eyes

were enucleated and homogenized in sterile PBS using stainless steel beads in a Tissue lyser (Qiagen, Valencia, CA). The homogenate was serially diluted in sterile PBS and plated on Tryptic Soy Agar (TSA) plates. The results were expressed as the mean number of CFU/eye ± SD.

Cytokine/Chemokine ELISA

The inflammatory cytokines and chemokines levels were measured using commercially available ELISA kits. Briefly, 15 µg of retinal lysate was used for the detection of mouse IL-6, IL-1β, TNF-α (BD Biosciences, San Jose, CA), CXCL-1, and MIP2 (CXCL-2) (R & D Systems, Minneapolis, MN) as per the manufacturer's instructions. The data are presented as the mean pg/mg of the retinal tissue lysate ± SD.

RNA extraction and real-time PCR analysis

Total RNA was extracted from the retinal tissue using TRIzol reagent following the manufacturer's instruction (Invitrogen, Carlsbad, CA). cDNA was synthesized using 1.0 µg of total RNA using a Maxima first-strand cDNA synthesis kit, as per the manufacturer's instructions (Thermo Scientific, Rockford, IL). qPCR was conducted in the StepOnePlus™ instrument (Applied Biosystem, Grand Island, NY) using cDNA for pro-inflammatory (*Tnf-α, Il-1β, Il-6*, *Cxcl-1* and *Cxcl-2*), anti-inflammatory (*Il-4, Il-10,* and *Tgf-β1*), M1 macrophage markers (*iNos, Il-23p19*, and *Il-12p40*), M2 macrophage markers (*Ym-1*, *Arg-1*, and *Fizz-1*), *Tlr2* and *Fpr2* genes. Primers were synthesized by Integrated DNA Technologies (Coralville, IA), and the oligonucleotide sequences are listed in **Table S2**. The gene expression levels were quantified using the comparative $\Delta\Delta^{CT}$ method. The expressions in the test samples were normalized to the endogenous reference actin levels. All the assays were performed in triplicate and were repeated at least twice.

Histological analysis.

The embedding, sectioning, and H&E staining were performed by Excalibur Pathology Inc. (Oklahoma City, OK).

Flow cytometry analysis

Flow cytometry was performed to assess neutrophil (PMN) infiltration in infected retinas[44, 50]. Briefly, following euthanasia, the retinas were isolated from the eyes and digested with Accumax (Millipore, Billerica, MA) for 10 min at 37°C. Retinas from two eyes were pooled together to obtain a sufficient number of cells. Following digestion, the retinal tissue was passed through a 23-gauge needle & syringe and filtered through a 40 µm cell strainer (BD Falcon, San Jose, CA). The cells were incubated with Fc Block (BD Biosciences, San Jose, CA) for 30 min, followed by a washing step with PBS containing 1% bovine serum albumin (BSA). Cells were then incubated with CD45-PECy5, Ly6G-FITC antibodies, and fixable viability dye eFLOUR 660 for 30 min in the dark. After subsequent washing steps, the cells were acquired on an Accuri C6 flow cytometer (BD Biosciences, San Jose, CA), and the data were analyzed using Accuri C6 software (BD Biosciences, San Jose, CA).

Analysis of retinal function.

Scotopic electroretinography (ERG) was performed to assess retinal function 6h following *S. aureus* infection and RvD1 treatment[50]. Briefly, all the mice (control, infected, and infected + RvD1 treated) were anesthetized 30h post SA-infection, maintained at 37°C using a heating pad, and the pupils were dilated using 1% tropicamide ophthalmic solution. ERGs were recorded following bilateral mydriasis and at least 4h of dark

adaptation. Silver-embedded thread eye electrodes (Ocuscience™ LLC, Kansas City, MO) were used to record the ERG. Reference needle electrodes (stainless steel subdermal needle electrodes) were placed in the anterior scalp, and a ground needle electrode was placed in the tail. ERG responses were acquired using an ERG system (Ocuscience™ LLC, Kansas City, MO) and analyzed using ERGVIEW 4.380V. Ganzfeld light stimulus was used to present ten 10ms flashes, with light intensities increasing from 0.0001 to 100 cd-s/m^2. The ERG a-wave was measured as amplitude between the ERG baseline and the first negative peak, and the ERG b-wave was measured as amplitude between the first negative peak and the first positive peak.

Plasmid preparation and cell transfection.

The mouse TLR2-HA (pUNO1-mTLR02-HA1x) and FPR2-DDK/FLAG (pCMV6-entry-mFPR2-Myc-DDK) plasmids were purchased from InvivoGen (San Diego, CA) and OriGene Technologies (Rockville, MD) respectively. The TLR2-HA and FPR2-DDK/FLAG plasmid were transformed in *E. coli* BL21 DE3 (Agilent Technologies, Santa Clara, CA). The recombinant clones were identified by PCR against *Tlr2* and *Fpr2* genes and used for plasmids preparation using the Maxiprep plasmid isolation kit (Qiagen, Valencia, CA). HEK293 cells (ATCC, Rockville, MD) were cultivated in DMEM media supplemented with 10% fetal bovine serum (FBS), 10 µg/ml L-glutamine, and 1% Penicillin & Streptomycin (Invitrogen, Carlsbad, CA). For transfection, HEK293 cells were plated in a 100mm petri dish and transfected with TLR2-HA and FPR2-DDK/FLAG (5µg each) either individually or in combination using Lipofectamine LTX PLUS reagent (Invitrogen, Carlsbad, CA). The transfection of TLR2 and FPR2 plasmids were confirmed by Western blot from HEK293-cell lysates using anti-HA and anti-FLAG/DDK antibodies, respectively.

Immunoprecipitation assay and Western blotting.

The TLR2-HA and FPR2-FLAG transfected HEK293 cells were washed with ice-cold PBS and lysed using RIPA buffer containing protease and phosphatase inhibitor cocktail (Thermo Fisher, Rockford, IL). The cell lysates were centrifuged at 12,000 x g for 20 min at 4ºC, and the total protein content of the resulting supernatant was determined using BCA (Thermo Fisher, Rockford, IL). To eliminate nonspecific binding during co-immunoprecipitation, the cell lysates were pre-cleared using mouse/rabbit IgG together with protein A/G PLUS agarose beads. A total of 200µg protein was incubated with 4µg/ml of anti-HA or anti-FLAG antibody overnight at 4ºC on a gyrorotatory shaker. Subsequently, the TLR2-HA and FPR2-FLAG proteins were pulled down using 20µl protein A/G PLUS agarose (Santa Cruz Biotechnology, Dallas, TX). The beads were rigorously washed five times with RIPA buffer containing protease and phosphatase inhibitors cocktail and eluted into 50µl of 1X SDS loading buffer. The crude lysate from the same assay was used as input controls. Western blotting was performed using standard SDS-PAGE and transfer methods [46, 85]. Briefly, total protein lysates were prepared by lysing cells in radioimmunoprecipitation assay (RIPA) buffer supplemented with protease and phosphatase inhibitor cocktails. Protein concentrations were determined using a Micro BCA™ protein assay kit (Thermo Scientific, Rockford, IL). Forty micrograms of protein were resolved on 8-12% SDS-PAGE and transferred onto a nitrocellulose membrane (0.45 µm) using a wet transfer system. Membranes were blocked with 5% (w/v) dry milk in Tris-buffered saline with Tween (TBST) for 1 hour at room temperature then incubated overnight at 4°C with primary antibodies (1:1000). After washing membranes were incubated with horseradish peroxidase (HRP)-conjugated

secondary antibodies (1:2000). After four washes with TBST, the membranes were developed using SuperSignal West Femto chemiluminescent substrate. Signals were captured using an iBright fluorescence imager (Thermo Scientific, Rockford, IL).

Phagocytosis assay

Phagocytosis and the intracellular killing assays were performed using retinal Müller glia (MIO-M1) cells as described previously[50] in the presence and/or absence of RvD1 and FPR2 inhibitors (WRW4 and PBP10). Briefly, MIO-M1 cells (10^6 cells/well) were grown in (60 mm) petri dishes in DMEM medium. The cells were treated with RvD1, PBP10, or WRW4 1h before infection. Subsequently, the cells were infected with *S. aureus* at a multiplicity of infection (MOI) of 10:1 in each petri dish and incubated for two hours. Following incubation, the cells were washed and treated with gentamicin (200µg/ml) for two hours to kill all extracellular and/or adherent bacteria. The absence of extracellular bacteria was confirmed via CFU enumeration on tryptic soy agar (TSA) plates. Two hours following the gentamicin addition, the cells were washed with DMEM and incubated in fresh DMEM containing gentamicin (200µg/ml) for 4h. For the internal killing assay, the cells were harvested 8h following incubation. For the enumeration of phagocytized and intracellular bacteria, following incubation, the cells were washed three times with PBS and lysed with 0.01% Triton X-100. The lysed cells were scraped and centrifuged at 5,000 x g for five minutes. The cell pellets were washed three times with PBS via centrifugation at 5,000 x g for 5 minutes. The pellets were then resuspended in 1 mL of sterile PBS. Serial dilutions were prepared, plated on TSA plates, and incubated overnight at 37°C. The next day, the colonies present on the TSA plates were counted, and counts were expressed as CFU/mL.

Statistics and reproducibility

All data are expressed as the mean ± SD unless indicated otherwise. Statistical differences between experimental groups were determined by one-way or two-way ANOVA. All statistical analyses are indicated in the figure legends, where ‘n’ represents the number of replicates. The number of replicates was determined based on our previous experiments/publications using these models. All statistical analyses were performed using GraphPad Prism (GraphPad Software, La Jolla, CA). A value of $P<0.05$ was considered statistically significant.

Data availability

All relevant data are included in the manuscript figures, supplementary information, and raw data points as supplementary files. Uncropped western blot images and the source data underlying all figures are provided as Supplementary Information. The source data behind the graphs are provided in supplementary data 1-11

Author Contributions

P.K.S. (Pawan Kumar Singh) conceived, designed, and performed the experiments, analyzed the data, and wrote the paper. S.S. (Sukhvinder Singh) and Aj.K. (Ajay Kumar) planned and performed the experiment, helped with the data analysis, graph preparation, and editing of the manuscript. S.G. (Shailendra Giri) provided intellectual input and edited the manuscript. A.K. (Ashok Kumar) conceived the idea and project administration, helped with the research planning, provided funding, and edited the manuscript. All the authors read and approved the final version of the manuscript.

Acknowledgments

This study is supported in part by the National Institute of Health (NIH)/National Eye Institutes (NEI) grants R01EY026964, R01EY027381, R01EY035499, and R21EY037082 to A.K. (Ashok Kumar) and R01EY032495 to P.K.S. This research is also supported in part by an unrestricted grant to the Kresge Eye Institute/Department of Ophthalmology, Visual, and Anatomical Sciences from Research to Prevent Blindness Inc. The immunology resource core is supported by an NIH Center grant P30EY004068. The funders had no role in the study design, data collection, interpretation, or decision to submit the work for publication. We thank Charles N. Serhan, PhD, DSc (Brigham and

Women's Hospital and Harvard Medical School, Boston, MA, USA), for his insightful discussions and expert guidance on bioactive lipid mediators.

Competing Interest

Authors declare no competing interests.

REFERENCES

1. Callegan, M. *et al.* Bacterial endophthalmitis: therapeutic challenges and host-pathogen interactions. *Prog Retin Eye Res* **26**, 189 - 203 (2007).

2. Durand, M.L. Endophthalmitis. *Clin Microbiol Infect* **19**, 227-234 (2013).

3. Cioana, M. *et al.* POSTINTRAVITREAL INJECTION AND POSTCATARACT EXTRACTION ENDOPHTHALMITIS VISUAL OUTCOMES BY ORGANISM: A SYSTEMATIC REVIEW AND META-ANALYSIS. *RETINA* **44** (2024).

4. Al Mahmood, A.M., Al-Swailem, S.A. & Behrens, A. Clear corneal incision in cataract surgery. *Middle East Afr J Ophthalmol* **21**, 25-31 (2014).

5. Almanjoumi, A.M., Combey, A., Romanet, J.P. & Chiquet, C. 23-gauge transconjunctival sutureless vitrectomy in treatment of post-operative endophthalmitis. *Graefes Arch Clin Exp Ophthalmol* **250**, 1367-1371 (2012).

6. Sadaka, A., Durand, M.L. & Gilmore, M.S. Bacterial endophthalmitis in the age of outpatient intravitreal therapies and cataract surgeries: Host-microbe interactions in intraocular infection. *Prog Retin Eye Res* **31**, 316-331 (2012).

7. Coburn, P.S. *et al.* Disarming Pore-Forming Toxins with Biomimetic Nanosponges in Intraocular Infections. *mSphere* **4** (2019).

8. Miller, F.C. *et al.* Targets of immunomodulation in bacterial endophthalmitis. *Prog Retin Eye Res* **73**, 100763 (2019).

9. Singh, S. *et al.* Integrative metabolomics and transcriptomics identifies itaconate as an adjunct therapy to treat ocular bacterial infection. *Cell reports. Medicine* **2**, 100277 (2021).

10. Singh, S. *et al.* Myeloid Cell-Specific Deletion of AMPKalpha1 Worsens Ocular Bacterial Infection by Skewing Macrophage Phenotypes. *J Immunol* **213**, 1656-1665 (2024).

11. Serhan, C.N., Chiang, N. & Van Dyke, T.E. Resolving inflammation: dual anti-inflammatory and pro-resolution lipid mediators. *Nature reviews. Immunology* **8**, 349-361 (2008).

12. Russell, C.D. & Schwarze, J. The role of pro-resolution lipid mediators in infectious disease. *Immunology* **141**, 166-173 (2014).

13. Jordan, P.M. & Werz, O. Specialized pro-resolving mediators: biosynthesis and biological role in bacterial infections. *The FEBS Journal* **289**, 4212-4227 (2022).

14. Yoo, S., Lim, J.Y. & Hwang, S.W. Resolvins: Endogenously-Generated Potent Painkilling Substances and their Therapeutic Perspectives. *Curr Neuropharmacol* **11**, 664-676 (2013).

15. Serhan, C.N. *et al.* Resolvins: a family of bioactive products of omega-3 fatty acid transformation circuits initiated by aspirin treatment that counter proinflammation signals. *J Exp Med* **196**, 1025-1037 (2002).

16. Serhan, C.N. *et al.* Anti-inflammatory actions of neuroprotectin D1/protectin D1 and its natural stereoisomers: assignments of dihydroxy-containing docosatrienes. *Journal of immunology* **176**, 1848-1859 (2006).

17. Duvall, M.G. & Levy, B.D. DHA- and EPA-derived resolvins, protectins, and maresins in airway inflammation. *Eur J Pharmacol* **785**, 144-155 (2016).

18. Rajasagi, N.K., Reddy, P.B., Mulik, S., Gjorstrup, P. & Rouse, B.T. Neuroprotectin D1 reduces the severity of herpes simplex virus-induced corneal immunopathology. *Invest Ophthalmol Vis Sci* **54**, 6269-6279 (2013).

19. Palmer, C.D. *et al.* 17(R)-Resolvin D1 differentially regulates TLR4-mediated responses of primary human macrophages to purified LPS and live E. coli. *J Leukoc Biol* **90**, 459-470 (2011).

20. Sulciner, M.L. *et al.* Resolvins suppress tumor growth and enhance cancer therapy. *J Exp Med* **215**, 115-140 (2018).

21. Ariel, A. *et al.* The docosatriene protectin D1 is produced by TH2 skewing and promotes human T cell apoptosis via lipid raft clustering. *J Biol Chem* **280**, 43079-43086 (2005).

22. Settimio, R., Clara, D.F., Franca, F., Francesca, S. & Michele, D. Resolvin D1 reduces the immunoinflammatory response of the rat eye following uveitis. *Mediators Inflamm* **2012**, 318621 (2012).

23. Hsiao, H.M. *et al.* A novel anti-inflammatory and pro-resolving role for resolvin D1 in acute cigarette smoke-induced lung inflammation. *PLoS One* **8**, e58258 (2013).

24. Mukherjee, P.K., Marcheselli, V.L., Serhan, C.N. & Bazan, N.G. Neuroprotectin D1: a docosahexaenoic acid-derived docosatriene protects human retinal pigment epithelial cells from oxidative stress. *Proc Natl Acad Sci U S A* **101**, 8491-8496 (2004).

25. Gronert, K. *et al.* A role for the mouse 12/15-lipoxygenase pathway in promoting epithelial wound healing and host defense. *J Biol Chem* **280**, 15267-15278 (2005).

26. Tang, Y. *et al.* Proresolution therapy for the treatment of delayed healing of diabetic wounds. *Diabetes* **62**, 618-627 (2013).

27. Levy, B.D. *et al.* Protectin D1 is generated in asthma and dampens airway inflammation and hyperresponsiveness. *Journal of immunology* **178**, 496-502 (2007).

28. Seki, H. *et al.* The anti-inflammatory and proresolving mediator resolvin E1 protects mice from bacterial pneumonia and acute lung injury. *Journal of immunology* **184**, 836-843 (2010).

29. El Kebir, D., Gjorstrup, P. & Filep, J.G. Resolvin E1 promotes phagocytosis-induced neutrophil apoptosis and accelerates resolution of pulmonary inflammation. *Proc Natl Acad Sci U S A* **109**, 14983-14988 (2012).

30. Kurihara, T. *et al.* Resolvin D2 restores neutrophil directionality and improves survival after burns. *Faseb J* **27**, 2270-2281 (2013).

31. Orr, S.K. *et al.* Unesterified docosahexaenoic acid is protective in neuroinflammation. *J Neurochem* **127**, 378-393 (2013).

32. Xu, Z.Z. *et al.* Neuroprotectin/protectin D1 protects against neuropathic pain in mice after nerve trauma. *Ann Neurol* **74**, 490-495 (2013).

33. Serhan, C.N. *et al.* Reduced inflammation and tissue damage in transgenic rabbits overexpressing 15-lipoxygenase and endogenous anti-inflammatory lipid mediators. *Journal of immunology* **171**, 6856-6865 (2003).

34. Mustafa, M. *et al.* Resolvin D1 protects periodontal ligament. *Am J Physiol Cell Physiol* **305**, C673-679 (2013).

35. Morita, M. *et al.* The lipid mediator protectin D1 inhibits influenza virus replication and improves severe influenza. *Cell* **153**, 112-125 (2013).

36. Serhan, C.N., Krishnamoorthy, S., Recchiuti, A. & Chiang, N. Novel anti-inflammatory--pro-resolving mediators and their receptors. *Current topics in medicinal chemistry* **11**, 629-647 (2011).

37. Ahmad, Z. *et al.* Untargeted and temporal analysis of retinal lipidome in bacterial endophthalmitis. *Prostaglandins Other Lipid Mediat* **171**, 106806 (2024).

38. Zhang, Q. *et al.* Specialized pro-resolving lipid mediators: a key player in resolving inflammation in autoimmune diseases. *Sci Bull (Beijing)* **70**, 778-794 (2025).

39. Kumar, A., Singh, P.K., Ahmed, Z., Singh, S. & Kumar, A. Essential Role of NLRP3 Inflammasome in Mediating IL-1β Production and the Pathobiology of Staphylococcus aureus Endophthalmitis. *Infection and immunity* **90**, e0010322 (2022).

40. Naik, P. *et al.* Multidrug-Resistant Pseudomonas aeruginosa Triggers Differential Inflammatory Response in Patients With Endophthalmitis. *Translational vision science & technology* **10**, 26 (2021).

41. Kumar, A., Singh, C.N., Glybina, I.V., Mahmoud, T.H. & Yu, F.S. Toll-like receptor 2 ligand-induced protection against bacterial endophthalmitis. *J Infect Dis* **201**, 255-263 (2010).

42. Singh, P.K., Donovan, D.M. & Kumar, A. Intravitreal Injection of the Chimeric Phage Endolysin Ply187 Protects Mice from Staphylococcus aureus Endophthalmitis. *Antimicrob Agents Chemother* **58**, 4621-4629 (2014).

43. Das, S., Singh, S. & Kumar, A. Bacterial Burden Declines But Neutrophil Infiltration and Ocular Tissue Damage Persist in Experimental Staphylococcus epidermidis Endophthalmitis. *Frontiers in cellular and infection microbiology* **11**, 780648 (2021).

44. Talreja, D., Singh, P.K. & Kumar, A. In Vivo Role of TLR2 and MyD88 Signaling in Eliciting Innate Immune Responses in Staphylococcal Endophthalmitis. *Invest Ophthalmol Vis Sci* **56**, 1719-1732 (2015).

45. Poisson, L.M. *et al.* Untargeted Plasma Metabolomics Identifies Endogenous Metabolite with Drug-like Properties in Chronic Animal Model of Multiple Sclerosis. *J Biol Chem* **290**, 30697-30712 (2015).

46. Singh, P.K. & Kumar, A. Retinal photoreceptor expresses toll-like receptors (TLRs) and elicits innate responses following TLR ligand and bacterial challenge. *PLoS One* **10**, e0119541 (2015).

47. Kochan, T., Singla, A., Tosi, J. & Kumar, A. Toll-like receptor 2 ligand pretreatment attenuates retinal microglial inflammatory response but enhances phagocytic activity toward Staphylococcus aureus. *Infection and immunity* **80**, 2076-2088 (2012).

48. Serhan, C.N. Pro-resolving lipid mediators are leads for resolution physiology. *Nature* **510**, 92-101 (2014).

49. Zhang, H. *et al.* The common promoter polymorphism rs11666254 downregulates FPR2/ALX expression and increases risk of sepsis in patients with severe trauma. *Crit Care* **21**, 171 (2017).

50. Singh, P.K., Shiha, M.J. & Kumar, A. Antibacterial responses of retinal Muller glia: production of antimicrobial peptides, oxidative burst and phagocytosis. *J Neuroinflammation* **11**, 33 (2014).

51. Shamsuddin, N. & Kumar, A. TLR2 mediates the innate response of retinal Muller glia to Staphylococcus aureus. *J Immunol* **186**, 7089-7097 (2011).

52. Singh, S., Singh, P.K. & Kumar, A. Butyrate Ameliorates Intraocular Bacterial Infection by Promoting Autophagy and Attenuating the Inflammatory Response. *Infect Immun* **91**, e0025222 (2023).

53. Francos-Quijorna, I. *et al.* Maresin 1 Promotes Inflammatory Resolution, Neuroprotection, and Functional Neurological Recovery After Spinal Cord Injury. *J Neurosci* **37**, 11731-11743 (2017).

54. Kilburg-Basnyat, B. *et al.* Specialized pro-resolving lipid mediators regulate ozone-induced pulmonary and systemic inflammation. *Toxicol Sci* (2018).

55. Fullerton, J.N., O'Brien, A.J. & Gilroy, D.W. Lipid mediators in immune dysfunction after severe inflammation. *Trends in Immunology* **35**, 12-21.

56. Leslie, M. Inflammation's stop signals. *Science* **347**, 18-21 (2015).

57. Rossi, S. *et al.* Protection from endotoxic uveitis by intravitreal Resolvin D1: involvement of lymphocytes, miRNAs, ubiquitin-proteasome, and M1/M2 macrophages. *Mediators Inflamm* **2015**, 149381 (2015).

58. Saban, D.R. *et al.* Resolvin D1 treatment on goblet cell mucin and immune responses in the chronic allergic eye disease (AED) model. *Mucosal Immunology* **12**, 145-153 (2019).

59. Gronert, K. Lipoxins in the eye and their role in wound healing. *Prostaglandins Leukot Essent Fatty Acids* **73**, 221-229 (2005).

60. He, J. *et al.* Lipoxin A4 (LXA4) Reduces Alkali-Induced Corneal Inflammation and Neovascularization and Upregulates a Repair Transcriptome. *Biomolecules* **13** (2023).

61. Wei, J. *et al.* A novel role for lipoxin A(4) in driving a lymph node-eye axis that controls autoimmunity to the neuroretina. *Elife* **9** (2020).

62. Mursalin, M.H. *et al.* C-X-C Chemokines Influence Intraocular Inflammation During Bacillus Endophthalmitis. *Invest Ophthalmol Vis Sci* **62**, 14 (2021).

63. Croasdell, A., Lacy, S.H., Thatcher, T.H., Sime, P.J. & Phipps, R.P. Resolvin D1 Dampens Pulmonary Inflammation and Promotes Clearance of Nontypeable Haemophilus influenzae. *Journal of immunology* **196**, 2742-2752 (2016).

64. Abdulnour, R.E. *et al.* Aspirin-triggered resolvin D1 is produced during self-resolving gram-negative bacterial pneumonia and regulates host immune responses for the resolution of lung inflammation. *Mucosal immunology* **9**, 1278-1287 (2016).

65. Norling, L.V. *et al.* Proresolving and cartilage-protective actions of resolvin D1 in inflammatory arthritis. *JCI Insight* **1**, e85922 (2016).

66. Novosad, B.D., Astley, R.A. & Callegan, M.C. Role of Toll-like receptor (TLR) 2 in experimental Bacillus cereus endophthalmitis. *PLoS One* **6**, e28619 (2011).

67. Ramadan, R.T., Ramirez, R., Novosad, B.D. & Callegan, M.C. Acute inflammation and loss of retinal architecture and function during experimental Bacillus endophthalmitis. *Curr Eye Res* **31**, 955-965 (2006).

68. Lee, J.E., Sun, Y., Gjorstrup, P. & Pearlman, E. Inhibition of Corneal Inflammation by the Resolvin E1. *Invest Ophthalmol Vis Sci* **56**, 2728-2736 (2015).

69. Krishnamoorthy, S., Recchiuti, A., Chiang, N., Fredman, G. & Serhan, C.N. Resolvin D1 receptor stereoselectivity and regulation of inflammation and proresolving microRNAs. *Am J Pathol* **180**, 2018-2027 (2012).

70. Recchiuti, A., Krishnamoorthy, S., Fredman, G., Chiang, N. & Serhan, C.N. MicroRNAs in resolution of acute inflammation: identification of novel resolvin D1-miRNA circuits. *Faseb J* **25**, 544-560 (2011).

71. Spite, M. *et al.* Resolvin D2 is a potent regulator of leukocytes and controls microbial sepsis. *Nature* **461**, 1287-1291 (2009).

72. Gordon, S. & Martinez, F.O. Alternative activation of macrophages: mechanism and functions. *Immunity* **32**, 593-604 (2010).

73. Chiang, N. *et al.* Infection regulates pro-resolving mediators that lower antibiotic requirements. *Nature* **484**, 524-528 (2012).

74. Norris, P.C. & Dennis, E.A. Omega-3 fatty acids cause dramatic changes in TLR4 and purinergic eicosanoid signaling. *Proc Natl Acad Sci U S A* **109**, 8517-8522 (2012).

75. Serhan, C.N., Chiang, N. & Van Dyke, T.E. Resolving inflammation: dual anti-inflammatory and pro-resolution lipid mediators. *Nat Rev Immunol* **8**, 349-361 (2008).

76. Koltsida, O. *et al.* Toll-like receptor 7 stimulates production of specialized pro-resolving lipid mediators and promotes resolution of airway inflammation. *EMBO Mol Med* **5**, 762-775 (2013).

77. Corminboeuf, O. & Leroy, X. FPR2/ALXR agonists and the resolution of inflammation. *J Med Chem* **58**, 537-559 (2015).

78. Jannaway, M., Torrens, C., Warner, J.A. & Sampson, A.P. Resolvin E1, resolvin D1 and resolvin D2 inhibit constriction of rat thoracic aorta and human pulmonary artery induced by the thromboxane mimetic U46619. *Br J Pharmacol* **175**, 1100-1108 (2018).

79. Nelson, J.W. *et al.* ALX/FPR2 receptor for RvD1 is expressed and functional in salivary glands. *Am J Physiol Cell Physiol* **306**, C178-185 (2014).

80. Chen, K. *et al.* Activation of Toll-like receptor 2 on microglia promotes cell uptake of Alzheimer disease-associated amyloid beta peptide. *J Biol Chem* **281**, 3651-3659 (2006).

81. Chen, K. *et al.* Cooperation between NOD2 and Toll-like receptor 2 ligands in the up-regulation of mouse mFPR2, a G-protein-coupled Abeta42 peptide receptor, in microglial cells. *J Leukoc Biol* **83**, 1467-1475 (2008).

82. Whiston, E.A. *et al.* alphaB-crystallin protects retinal tissue during Staphylococcus aureus-induced endophthalmitis. *Infection and immunity* **76**, 1781-1790 (2008).

83. Maddipati, K.R. *et al.* Eicosanomic profiling reveals dominance of the epoxygenase pathway in human amniotic fluid at term in spontaneous labor. *Faseb J* **28**, 4835-4846 (2014).

84. Maddipati, K.R. & Zhou, S.L. Stability and analysis of eicosanoids and docosanoids in tissue culture media. *Prostaglandins & other lipid mediators* **94**, 59-72 (2011).

85. Singh, P.K. *et al.* Zika virus infects cells lining the blood-retinal barrier and causes chorioretinal atrophy in mouse eyes. *JCI Insight* **2**, e92340 (2017).

FIGURES and LEGENDS.

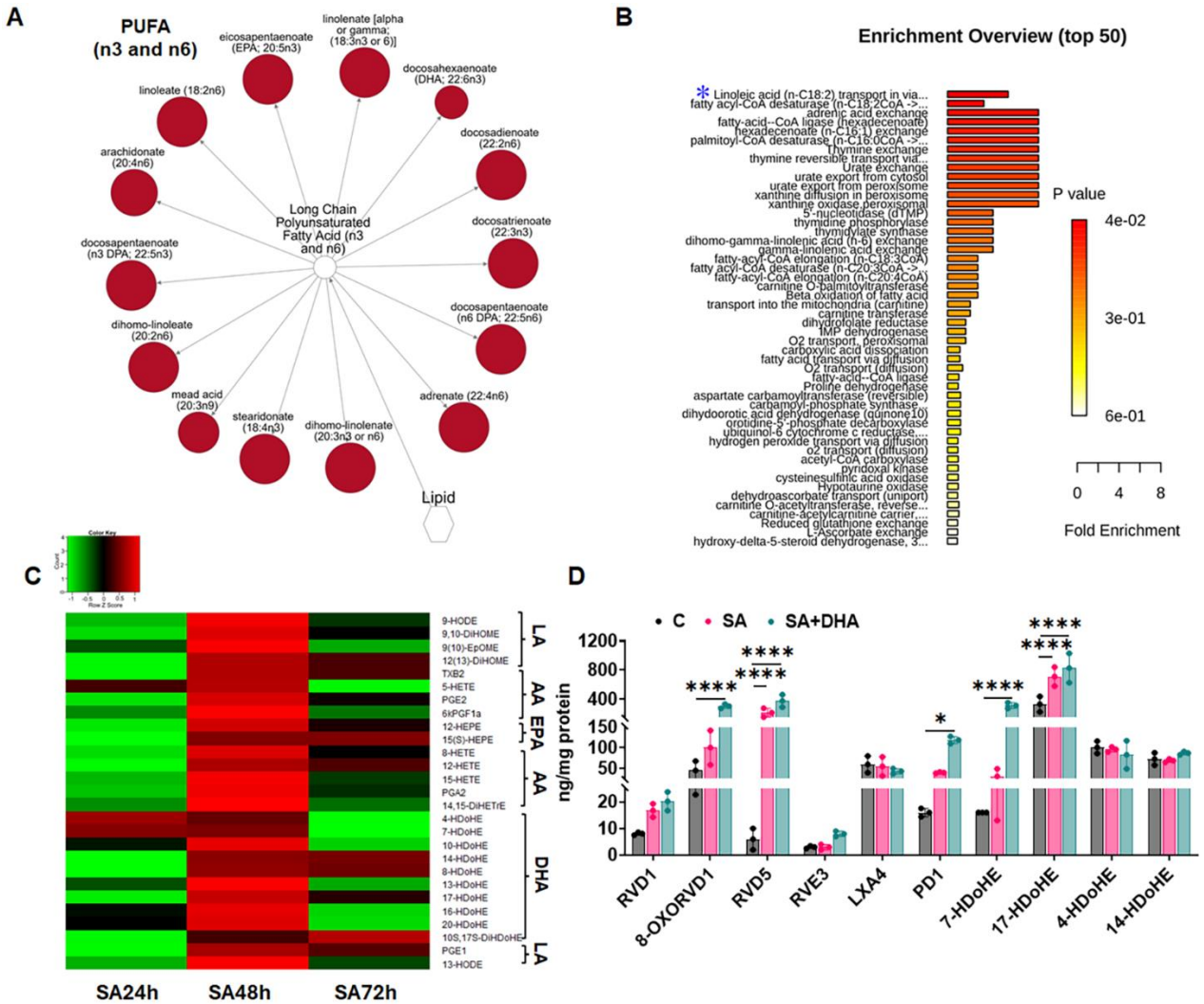

Figure 1: Metabolomics and lipidomics analysis reveal the production of SPMs during endophthalmitis. C57BL/6 mice were injected intravitreally with the *S. aureus* (SA) strain RN6390 (5000 CFU/eye) with PBS-injected eyes as controls. Retinal tissues at 24, 48 and 72h post-SA infection were harvested and subjected to metabolomics (**A & B**) and lipidomics (**C & D**) analysis. Interactive network analysis showed dysregulation of lipids and n3 and n6 PUFAs at 72h timepoint (**A**). Pathway enrichment analysis showing the top 50 dysregulated metabolic pathways (**B**). Heatmap showing differential changes in SPMs and their intermediates in SA-SA-infected retina (**C**). In another set of experiments, DHA (100 ng/eye) was administered via intravitreal injection 24h post-SA infection, and eyes were enucleated 6h post-DHA injections (i.e., 30h of infection). The bar graphs indicate the induction of SPMs and their intermediates in DHA-treated groups (**D**). Error bars: mean ± SD, ∗ p<0.05, ∗∗ p<0.005, ∗∗∗∗ p<0.0001, ANOVA.

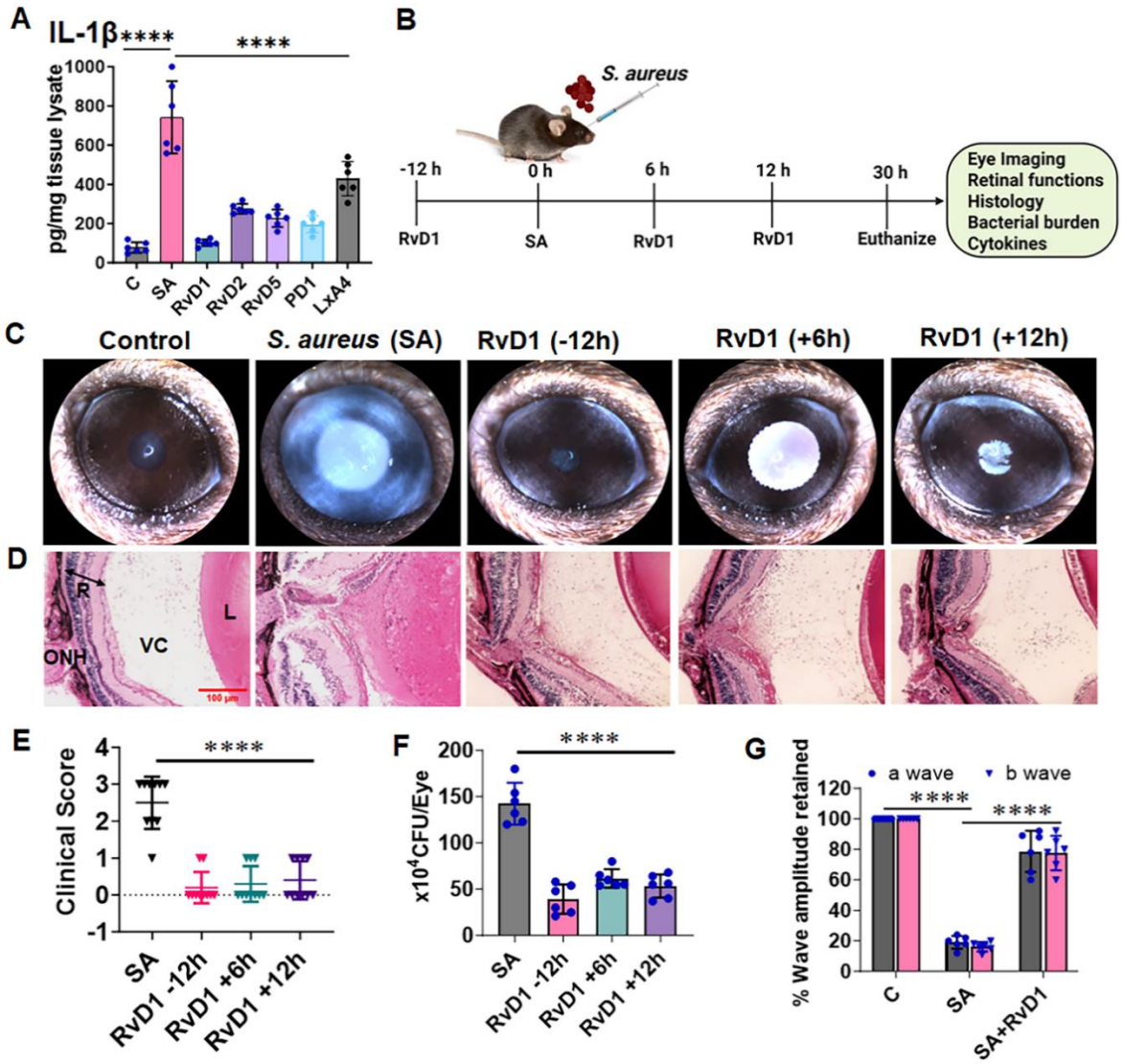

Figure 2: RvD1 treatment ameliorates *S. aureus* endophthalmitis in mice. C57BL/6 mice (n=6) were injected intravitreally with *S. aureus* (SA) strain RN6390 (5000CFU/eye). SA-infected eyes were treated with listed bioactive lipid mediators 6h post-infection, and retinal tissue was used for IL-1β ELISA **(A)**. The SA-infected eyes were either pre (-12h before infection) or post- (+6h or +12h post-infection) treated with RvD1 as per the given timeline, and all assays were performed at 30h post SA infection **(B,** created using https://www.biorender.com/). Clinical examination was performed, and eye images were taken using an ophthalmoscope with an attached camera **(C)**. For histological analysis, eyes were enucleated and subjected to H&E staining (scale bar, 100 µm) **(D)**. Individual eyes were assigned clinical scores (range 0 to 4), and the data are presented as the mean clinical scores **(E)**. For bacterial burden, the eyes were enucleated, homogenized, and the bacterial burden was estimated via serial dilution plating **(F)**. For visual function testing, ERG responses to a 6-dB flash were recorded. The percentage amplitudes of the a- and b-waves retained in 6h post-RvD1-treated group and untreated mice were compared to those of uninfected controls **(G)**. Error bars: mean ± SD, ****p<0.0001, ANOVA. R: retina, ONH: optic nerve head, VC: vitreous chamber, L: lens.

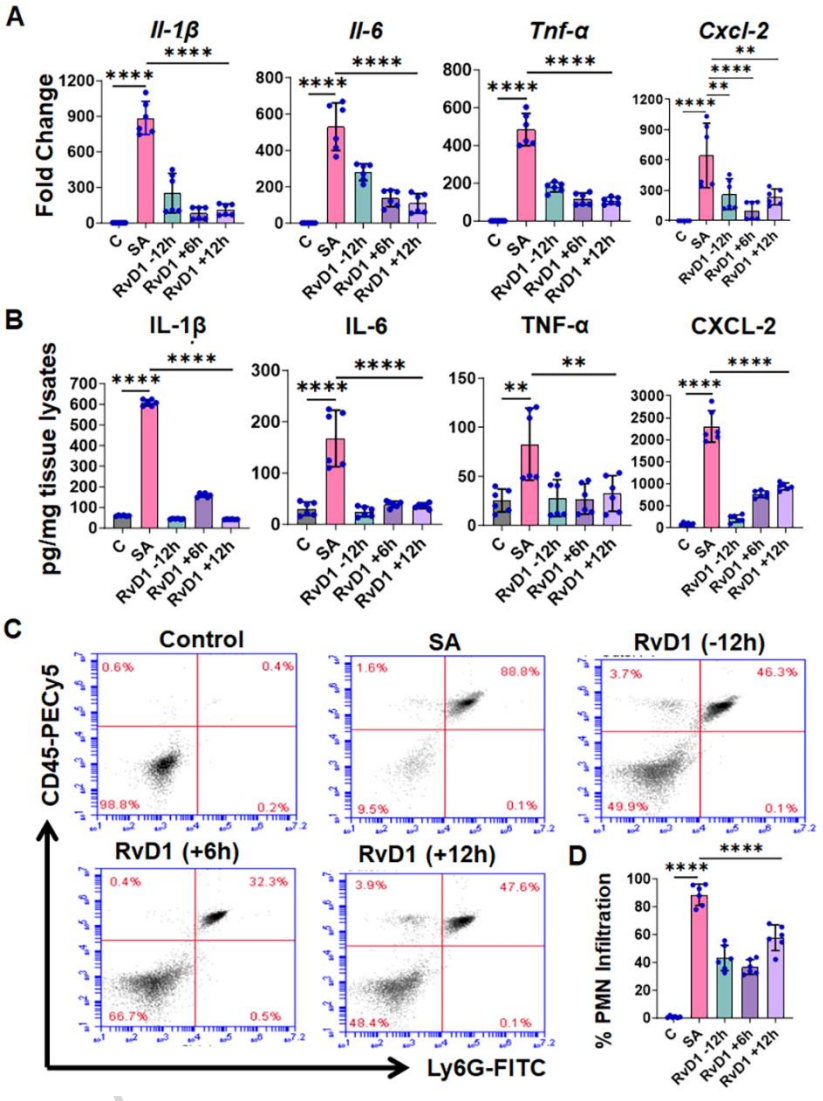

Figure 3: RvD1 reduces SA-induced inflammation and PMN infiltration. C57BL/6 mice (n=6/group) were injected intravitreally with *S. aureus* (SA) strain RN6390 (5000 CFU/eye). The SA-infected eyes were either pre- (-12h before infection) or post- (+6h or +12h post-infection) treated with RvD1. Thirty hours post-SA infection, retinal tissues were harvested and subjected to qPCR for indicated cytokines/chemokines **(A)**. To measure protein levels, eyes were enucleated, and 10µg protein lysate was used for the detection of indicated inflammatory cytokines/chemokines by ELISA **(B)**. ** p<0.005; ****p<0.0081, ANOVA. In a second set of experiments, RvD1-treated and untreated eyes were enucleated, and the retina/vitreous from two eyes were pooled to make single-cell suspensions for flow cytometry analysis. The cells were stained with anti-CD45-PECy5 and anti-Ly6G-FITC antibodies. Post-acquisition, the cells were size-gated to differentiate them from debris. The percentage of dually positive PMNs was determined using a CD45 vs. Ly6G dot plot **(C & D)**. Error bars: mean ± SD, ** p<0.005, ****p<0.0001, ANOVA.

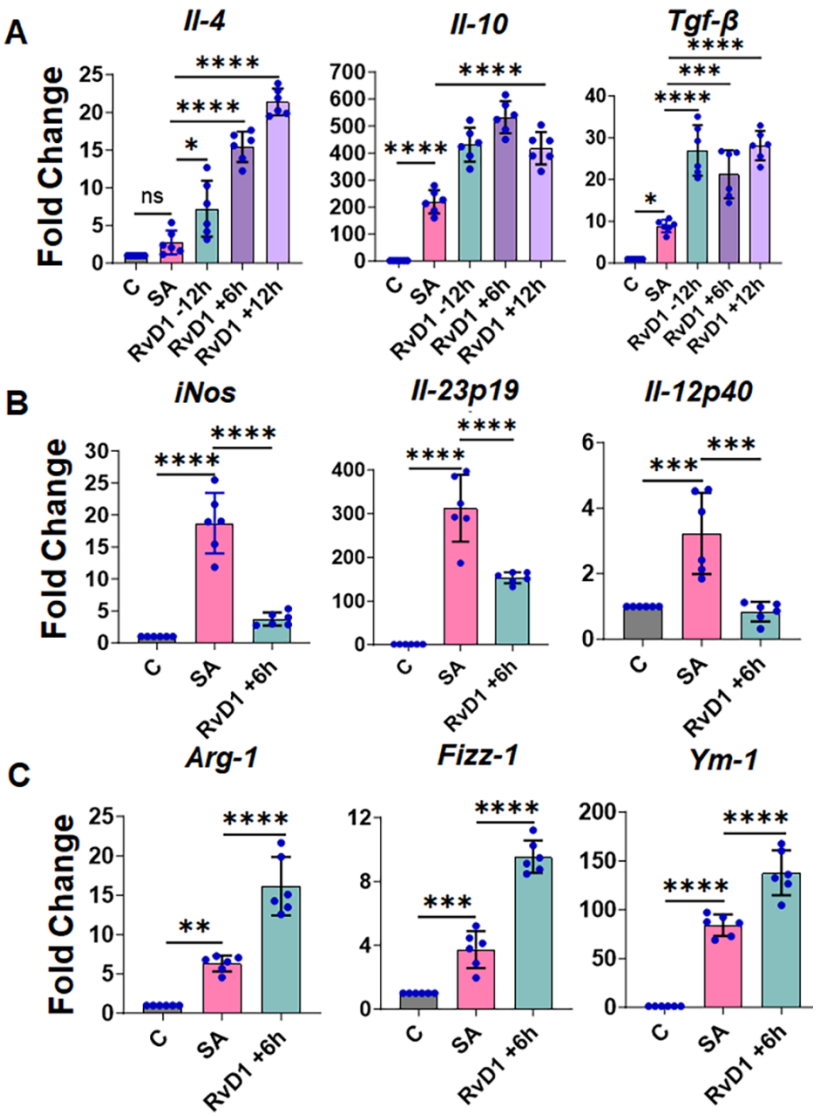

Figure 4: RvD1 induces anti-inflammatory mediators and promotes M2 macrophage/microglia class switching. C57BL/6 mice (n=6/group) were injected intravitreally with *S. aureus* (SA) strain RN6390 (5000CFU/eye). The SA-infected eyes were either pre (-12h before infection) or post- (+6h or +12h post-infection) treated with RvD1. Thirty hours post-SA infection, retinal tissues were harvested and subjected to qPCR for indicated anti-inflammatory **(A),** M1 macrophage **(B),** and M2 macrophage **(C)** phenotype markers. Error bars: mean ± SD, ns=not significant, ∗p<0.05; ∗∗p<0.005; ∗∗∗p<0.0005, ∗∗∗∗p<0.0001, ANOVA.

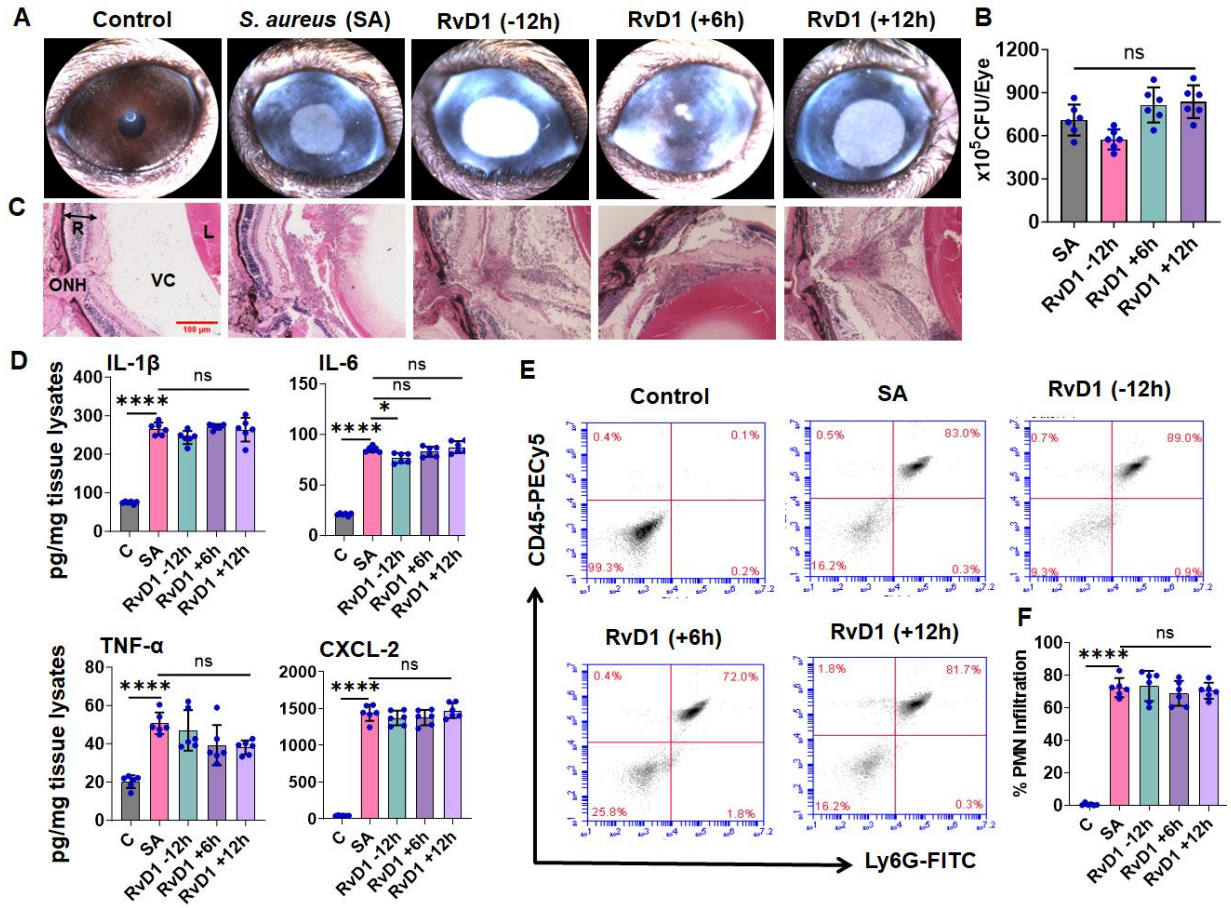

Figure 5: RvD1 failed to promote inflammation resolution and ameliorate endophthalmitis in TLR2-deficient mice. TLR2$^{-/-}$ mice (n=6) were injected intravitreally with *S. aureus* (SA) strain RN6390 (5000 CFU/eye). The SA-infected eyes were either pre (-12h before infection) or post- (+6h or +12h post-infection) treated with RvD1 and all assays were performed at 30h post SA infection. Clinical examination was performed, and micrographs were taken from representative eyes using an ophthalmoscope mounted with a camera **(A)**. For bacterial burden, the eyes were enucleated, homogenized, and the bacterial burden was estimated via serial dilution plating **(B).** For histological analysis, eyes were enucleated and subjected to H&E staining (scale bar, 100 µm) **(C)**. Eyes were enucleated, and 10µg protein lysate was used for the detection of indicated inflammatory cytokines/chemokines by ELISA **(D)**. PMN infiltration was measured using flow cytometry following anti-CD45-PECy5 and anti-Ly6G-FITC staining **(E)** and presented as a bar graph **(F)**. Error bars: mean ± SD, ns=not significant, ∗p<0.05; ∗∗∗∗p<0.0001, ANOVA. R: retina, ONH: optic nerve head, VC: vitreous chamber, L: lens.

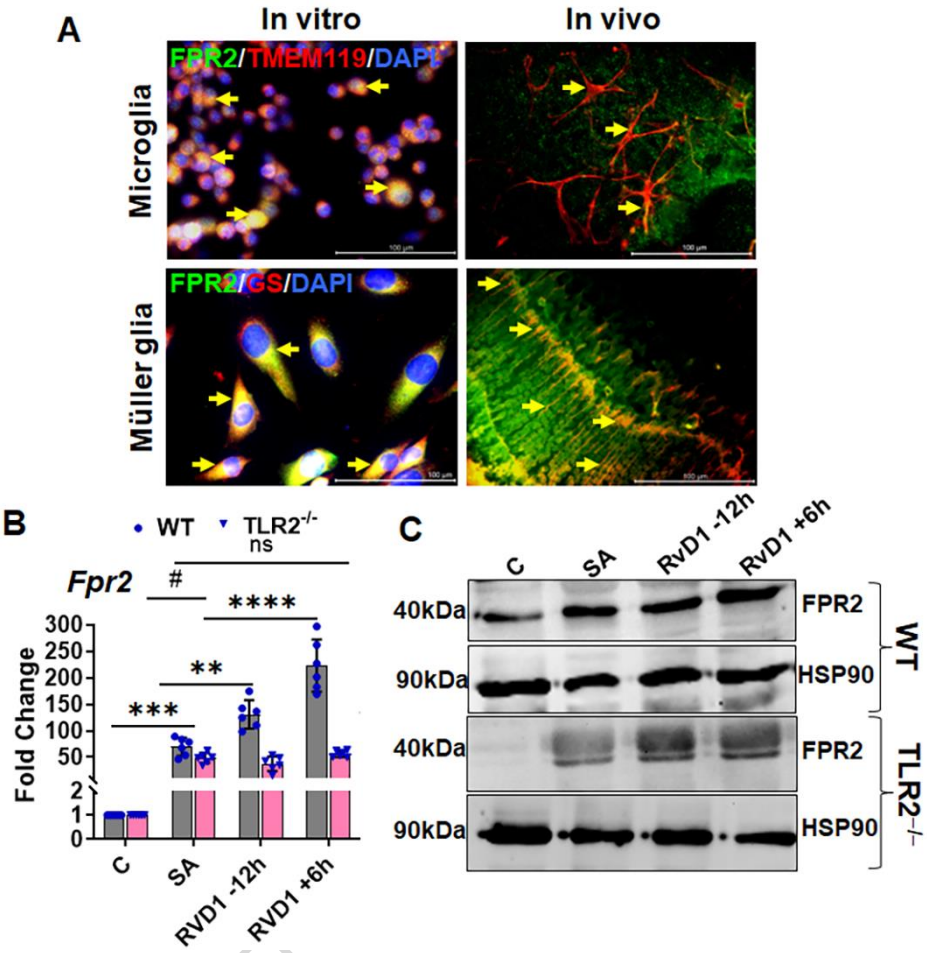

Figure 6: Müller glia and microglia express FPR2, and RvD1 potentiates its expression in the retina. (A, left panels) Mouse microglial (BV2 cell line), and human Müller glia (MIO-M1 cell line) were cultured and co-immunostained with FPR2, TMEM119 (microglial marker), or GS (Müller glia marker). C57BL/6 mice (n=4/group) were injected intravitreally with *S. aureus* (SA) strain RN6390 (5000CFU/eye) and 24h later, retinal flat mount or cryosections were prepared and subjected to immunostaining for FPR2-TMEM119 (microglia) and FPR2-GS (Müller glia) (scale bar, 100 µm) **(A, right panels)**. A few representative areas highlighted with yellow arrows indicate co-localization, scale bar: 100µm. Retina from C57BL/6 WT and TLR2$^{-/-}$ mice (n=6) following *S. aureus* infection and RvD1 treatment were subjected to qPCR **(B)** and western blot **(C)** analysis of FPR2 and HSP90**.** Error bars: mean ± SD, ns=not significant, #, ∗p<0.05; ∗∗p<0.005; ∗∗∗p<0.0005, ∗∗∗∗p<0.0001, ANOVA (∗ WT: C vs. SA and $^{\#}$SA vs. RvD1).

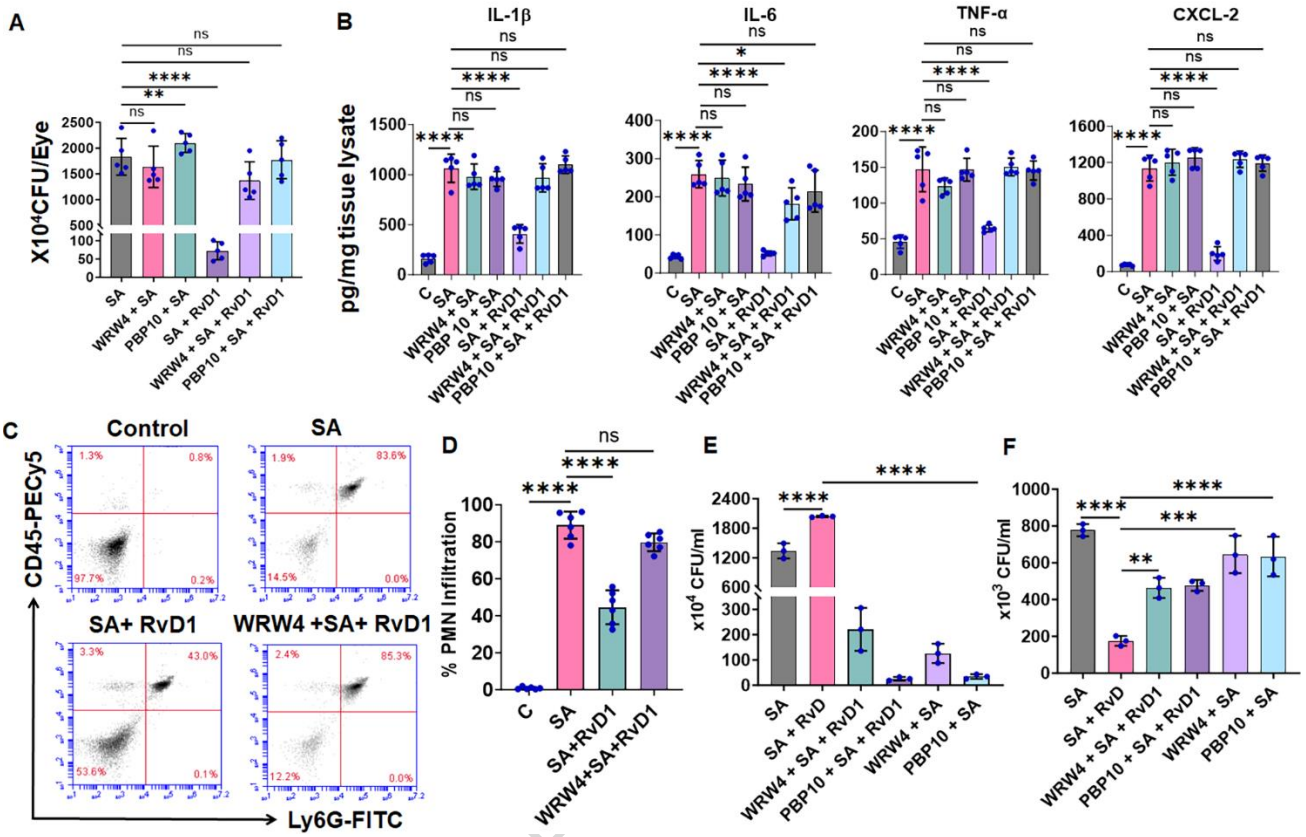

Figure 7: FPR2 inhibition attenuated RvD1-mediated protection in B6 mice. C57BL/6 mice (n=6/group) were intravitreally injected with FPR2 antagonist WRW4 and PB10. Twelve hours following inhibitor injection, mice were infected intravitreally with *S. aureus* (SA) strain RN6390 (5000 CFU/eye) and treated with RvD1 6h following infection. SA alone and SA with inhibitors were used as controls. Thirty hours post SA-infection, the bacterial burden in infected vs treated eyes was enumerated by serial dilution and plate count method **(A)**. The cytokines/chemokine levels **(B)** and the PMN infiltration **(C & D)** were measured using ELISA and flow cytometry, respectively. For phagocytosis and internal killing assay, retinal Müller glia, MIO-M1 cells, were treated with RvD1 in the presence and absence of FPR2 antagonists WRW4 or PBP10, as described in the methods section. The bacterial counts were enumerated following cell lysis, washing, and dilution plating, 4h following incubation for phagocytosis assay (n=3) **(E),** and 8h following incubation for internal killing assay (n=3) **(F)**. Error bars: mean ± SD, ns=not significant, ∗p<0.05; ∗∗p<0.005; ∗∗∗∗p<0.0001, ANOVA.

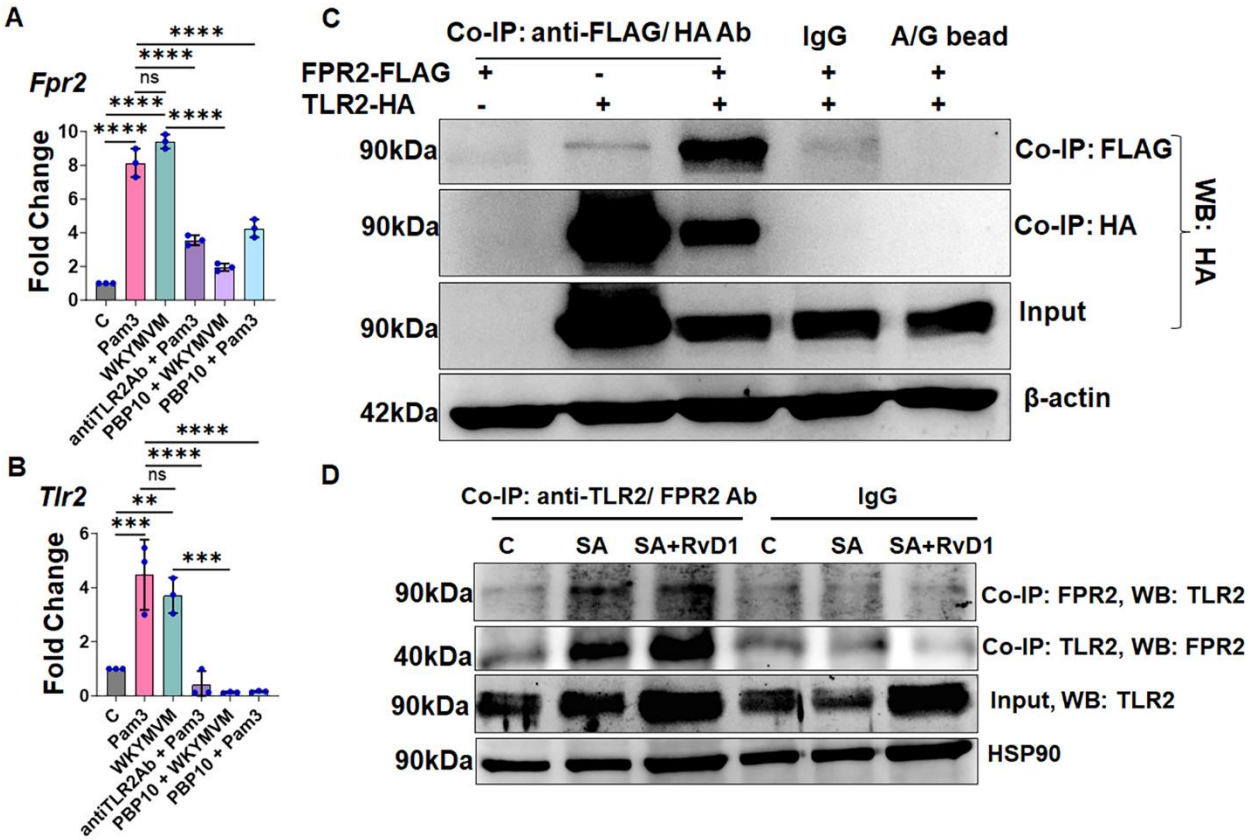

Figure 8: FPR2 and TLR2 regulate their mutual expression and interaction. C57BL/6 mice (n=3/group) were intravitreally injected with FPR2 agonist WKYMVM and TLR2 agonist Pam3 with and without FPR2 antagonist PB10 (PBP10 was injected 12h before WKYMVM and Pam3 injections in inhibition groups). Twenty-four hours following injection, the retinas were harvested and subjected to qPCR for *Fpr2* **(A)** and *Tlr2* **(B)** genes. Error bars: mean ± SD, ns=not significant, ∗∗p<0.005; ∗∗∗p<0.0005, ∗∗∗∗p<0.0001, ANOVA. HEK293 cells were transfected with TLR2-HA and/or FPR2-DDK/FLAG plasmids. Twenty-four hours following transfection, precleared protein lysates were co-immunoprecipitated (Co-IP) using anti-HA and anti-FLAG antibodies, followed by Western blot using anti-FLAG and anti-HA antibodies, respectively. Isotype mouse IgG and A/G agarose beads were used as controls to examine the specificity of Co-IP. The crude protein lysates were used as input control **(C)**. C57BL/6 mice were intravitreally infected with *S. aureus* RN6390 (5000 CFU/eye) and treated with RvD1 at 6h post-infection. Uninfected control, SA-infected, and RvD1-treated retinal lysates were used for Co-IP using anti-TLR2/anti-FPR2 antibodies, followed by western blotting for anti-FPR2/anti-TLR2 antibodies, respectively. Crude retinal lysates were used as an input control **(D)**.

Editor's Summary

RvD1 protects against *Staphylococcus aureus* endophthalmitis by bacterial clearance, intraocular inflammation reduction, and retinal function preservation through the TLR2–FPR2 signalling crosstalk.

Peer review statement

Communications Biology thanks Phillip S. Coburn and the other, anonymous, reviewer(s) for their contribution to the peer review of this work. Primary Handling Editor: Dario Ummarino.